Spatially segregated transcription and translation in cells of the endomembrane-containing bacterium *Gemmata obscuriglobus*

Ekaterina Y. Gottshall, Corrine Seebart, Jesse C. Gatlin, and Naomi L. Ward[1]

Department of Molecular Biology, University of Wyoming, Laramie, WY 82071

Edited by Nancy A. Moran, University of Texas at Austin, Austin, TX, and approved June 27, 2014 (received for review May 21, 2014)

The dogma of coupled transcription and translation in bacteria has been challenged by recent reports of spatial segregation of these processes within the relatively simple cellular organization of the model organisms *Escherichia coli* and *Bacillus subtilis*. The bacterial species *Gemmata obscuriglobus* possesses an extensive endomembrane system. The membranes generate a very convoluted intracellular architecture in which some of the cell's ribosomes appear to have less direct access to the cell's nucleoid(s) than others. This observation prompted us to test the hypothesis that a substantial proportion of *G. obscuriglobus* translation may be spatially segregated from transcription. Using immunofluorescence and immunoelectron microscopy, we showed that translating ribosomes are localized throughout the cell, with a quantitatively greater proportion found in regions distal to nucleoid(s). Our results extend information about the phylogenetic and morphological diversity of bacteria in which the spatial organization of transcription and translation has been studied. These findings also suggest that endomembranes may provide an obstacle to colocated transcription and translation, a role for endomembranes that has not been reported previously for a prokaryotic organism. Our studies of *G. obscuriglobus* may provide a useful background for consideration of the evolutionary development of eukaryotic cellular complexity and how it led to decoupled processes of gene expression in eukaryotes.

Transcription and translation mechanisms are highly conserved across the Tree of Life, but their spatial organization distinguishes prokaryotes from eukaryotes. Prokaryotic coupling of transcription and translation is possible because bacteria lack a physical barrier (nuclear membrane) between the two processes. Coupling allows increased mRNA stability and translational regulation of transcription (1). Although it is facilitated by colocalization of ribosomes and nucleoid (2), as seen in the model organism *Caulobacter crescentus* (3), colocalization is not universal (4–6). In both *Bacillus subtilis* (4) and *Escherichia coli* (4–6) there is considerable spatial segregation between RNA polymerase (RNAP), which is restricted to the nucleoid, and some of the cell's ribosomes. However, relatively small distances between RNAP and most ribosomes (7), intrinsic signals that target mRNA to the cell poles (8), and mRNA chaperone mechanisms (4–6) allow coupling in the absence of colocalization. Beyond these three model species with their relatively simple cellular architecture, the spatial organization of transcription and translation within the enormous diversity of the Bacteria is not well understood.

The planctomycete bacterial species *Gemmata obscuriglobus* possesses an extensive endomembrane network (9–18). Endocytosis-like behavior (15, 19) suggests that cellular transport may be a primary function of the endomembrane network. On the basis of transmission electron microscopy (TEM), these membranes originally were proposed to be unique to the organism and distinct from the cytoplasmic membrane, forming compartments that enclose the cell's nucleoid(s) (10–13). More recent electron tomography studies (14, 16–18) support (18) or refute (14, 16, 17) this interpretation. The studies of Acehan et al. (16) and Santarella-Mellwig et al. (17) suggest that the endomembranes constitute a highly invaginated cytoplasmic membrane (and thus an extension of the typical Gram-negative cell plan) and that cytoplasmic volumes are all interconnected. These conflicting interpretations support conflicting opinions about the evolutionary relationship of *G. obscuriglobus* to eukaryotes (20–22). Regardless of its evolutionary history, the complex endomembrane network creates a unique cellular context for the spatial organization of gene expression. The convoluted cytoplasm contains some ribosome-like particles that are immediately adjacent to nucleoid(s), but others are spatially distant. However, although these particles are identified as ribosomes through RNase-gold labeling (13), it is unclear whether active ribosomes are restricted to certain regions, as previously reported for *C. crescentus* (3). This uncertainty, together with a previous proposal (12) that some translation may be uncoupled from transcription, led us to test the hypothesis that a substantial proportion of *G. obscuriglobus* translation may be spatially segregated from transcription.

Results

TEM Confirms the Presence of a Complex Endomembrane System in Cells of *G. obscuriglobus*. Because the cellular architecture of *G. obscuriglobus* is variable and dynamic (10, 14, 16, 17), we performed TEM to compare the ultrastructure of cells from our cultures with that reported previously. We observed the characteristic endomembrane system (single- and double-layered membranes), condensed nucleoid(s), and many regions distal to

Significance

Eukaryotic (plant and animal) cells possess a nuclear membrane that separates the two stages of gene expression (transcription and translation), whereas prokaryotic (bacteria and archaea) cells lack the nuclear membrane barrier to colocated transcription and translation. However, cells of the bacterium *Gemmata obscuriglobus* possess extensive intracellular membranes, resulting in superficially eukaryote-like cellular complexity. We have found that a substantial amount of *G. obscuriglobus* translation is uncoupled from transcription, broadening our understanding of the spatial organization of bacterial gene expression, which currently is based entirely on a handful of model species. This broader understanding provides a useful background for consideration of the evolutionary development of eukaryotic cellular complexity and how it led to decoupled processes of gene expression in eukaryotes.

Author contributions: E.Y.G., C.S., J.C.G., and N.L.W. designed research; E.Y.G. and C.S. performed research; E.Y.G., C.S., J.C.G., and N.L.W. analyzed data; and E.Y.G., C.S., J.C.G., and N.L.W. wrote the paper.

The authors declare no conflict of interest.

This article is a PNAS Direct Submission.

[1]To whom correspondence should be addressed. Email: nlward@uwyo.edu.

This article contains supporting information online at www.pnas.org/lookup/suppl/doi:10.1073/pnas.1409187111/-/DCSupplemental.

the cell's nucleoid(s) (Fig. 1), as previously reported for 2D imaging (10, 11, 13). Because we were limited to 2D approaches, we could not interpret the topology of cell features such as nucleoids (that appear as single or multiple nucleoids in 2D images) or the degree of connectivity of cellular regions and membranes (16, 17).

Specific Detection of *G. obscuriglobus* Transcription and Translation Proteins Through Western Blotting of Whole-Cell Lysates. Genetic manipulation of *G. obscuriglobus*, which would permit tagging to be used for protein localization, is not yet possible; therefore immunological detection is the only currently available method. We tested both commercially available and custom antibodies for their ability to detect *G. obscuriglobus* proteins specifically involved in transcription and translation and hence their suitability for localization experiments. RNAP and ribosomal subunit S10 (hereafter, S10) were chosen as markers for transcription and the ribosome, respectively, and transcription factor N-utilization factor G (NusG) served as an indicator of both transcription and translation. Elongation factor Tu (EF-Tu) was selected as a marker of active protein synthesis, because it is an essential component for nascent peptide elongation (23, 24) and can bind only to an assembled ribosome (25). A commercially available antibody against *E. coli* RNAP β subunit (RNAP-β) and custom antibodies raised against *G. obscuriglobus* S10, EF-Tu, and NusG detected single bands of the expected size (150, 13, 47, and 27 kDa, respectively) in Western blots of *G. obscuriglobus* whole-cell lysates (Fig. S1).

Anti-S10 and anti–EF-Tu Antibodies Bind to Ribosomes Isolated from *G. obscuriglobus*. To confirm the binding of primary antibodies to ribosomes, we isolated ribosomal fractions from *G. obscuriglobus* and *E. coli* and tested for enrichment of immunoreactive signal. Successful ribosomal enrichment was demonstrated by the presence of RNase-sensitive nucleic acid bands corresponding in size to the 23S and 16S rRNAs (2.9 and 1.5 Kb, respectively), in both the crude pellet (P1) and cytosolic ribosome (P2) fractions (Fig. S2*A*). The P1 and P2 fractions also contained proteins with migration properties characteristic of ribosomal proteins (Fig. S2*B*) (26), although some *G. obscuriglobus* proteins may differ in size from those in *E. coli* (Fig. S3). The ability of our custom anti-S10 and anti–EF-Tu antibodies to detect *G. obscuriglobus* ribosomes was determined by Western blot analysis of the subcellular fractions (Fig. S4), with total protein load normalized in each lane (Bradford assay). The anti-S10 antibody yielded signal against the P2 fraction, with a weaker signal (possibly arising from membrane-bound ribosomes) detected in the P1 fraction. Further analysis suggested that the anti-S10 signal was 15–20 times greater in P2 than in P1 (Fig. S5). The anti–EF-Tu antibody signal was present in all subcellular fractions with an apparent enrichment in P1 (Fig. S4); EF-Tu may have this relatively broad distribution because it is not permanently bound to the ribosome.

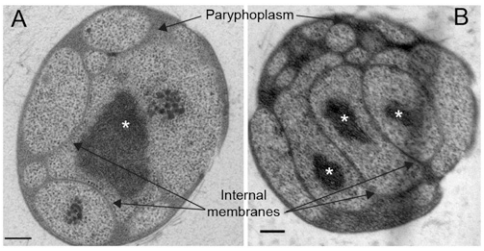

Fig. 1. Complex endomembrane system in cells of *G. obscuriglobus*. TEM images are representative of at least 20 cells. Arrows indicate paryphoplasm/periplasm and internal membranes. Nucleoid(s) are labeled with asterisks. The image in *A* suggests that relatively large expanses of peripheral cytoplasm are distant from the nucleoid(s). A prominent internal membrane in *A* appears to be double-layered and to carry bound ribosomes, as previously reported (10). With the 2D approaches used in this study, some cells appear to have a single nucleoid (*A*), and others have multiple nucleoids (*B*). However, it is difficult to determine nucleoid number accurately in the absence of 3D data. A cell that appears to contain only one nucleoid (*A*) may in fact harbor another that is not visible in this thin section, whereas the appearance of multiple nucleoids (*B*) may result from capturing multiple lobes of a single nucleoid in one section. (Scale bars: 200 nm.)

Evidence for Translating Ribosomes Throughout the *G. obscuriglobus* Cell. To determine the cellular location of actively translating *G. obscuriglobus* ribosomes, we used immunofluorescence microscopy with primary antibodies targeting S10 and EF-Tu and dyes binding DNA (DAPI) and membranes (3,3′-dihexyloxacarbocyanine iodide; DiOC6). S10 and EF-Tu exhibited punctate distribution both proximal to and distant from the cell's nucleoid(s), with a qualitatively greater abundance in distant regions (peripheral areas lacking DAPI signal; Fig. 2 *A* and *B*). To exclude the possibility that the apparent S10 and EF-Tu enrichment in nucleoid-distal regions was caused by reduced access of the antibodies to nucleoid-proximal regions, we also examined the distribution of NusG. This protein interacts with both RNAP and S10 (27) and therefore should be found both tightly associated with the nucleoid(s) and colocalized with the cell's ribosomes, including those distant from the nucleoid(s); we observed the expected distribution (Figs. S6 and S7*D*).

Quantitative Colocalization Analysis of DNA and Translation Markers Suggests Enrichment of Translating Ribosomes in Regions Distant from the Nucleoid(s). We performed colocalization analysis of fluorescent signal for individual cells of *G. obscuriglobus* treated with anti-S10, anti–EF-Tu, and anti-NusG antibodies and stained with DAPI and DiOC6. Pearson correlation coefficients (*Rr*) (28) were calculated for each pair of fluorescent signals within an individual cell. In all images the background fluorescence was subtracted to reduce its effect on colocalization estimations. Based on the use of 0.5 as an *Rr* threshold for positive colocalization (29), neither the anti-S10 nor the anti–EF-Tu signal was completely colocalized with DAPI signal (Fig. 2 *C* and *D*). However, ∼50% of cells showed *Rr* values greater than zero, representing some degree of signal overlap. In both cell populations examined—anti-S10 and anti–EF-Tu—*Rr* values for DAPI and DiOC6 colocalization were almost all negative (Fig. S7*A*), serving as a negative control for colocalization. In contrast, the majority of values obtained for ribosome-targeting antibodies and DiOC6 were positive (Fig. S7*B*) and served as a colocalization positive control, chosen because blot data from cell fractionation were consistent with a fraction of *G. obscuriglobus* ribosomes being membrane bound (Fig. S5). To verify that the EF-Tu signal corresponds to actively translating ribosomes, cells were treated with the translation inhibitor chloramphenicol at a concentration of 100 μg/mL. DNA and EF-Tu appeared to be more colocalized (Fig. S7*C*) after translation was inhibited, showing that EF-Tu localization has shifted, possibly because EF-Tu has a lower affinity for nontranslating ribosomes. Last, quantification of the NusG-DAPI signal yielded a correlation of ∼0.4 (Fig. S7*D*), consistent with a distribution of NusG both close to and far from, the nucleoid. This result supports our assertion that cellular regions close to the nucleoid(s) are accessible to the anti-S10 and anti–EF-Tu primary antibodies and that their lack of colocalization with DAPI signal is not caused by inaccessibility.

The *G. obscuriglobus* RNAP-β Subunit Is Restricted to the Nucleoid(s) and Is Located in Foci. The location of RNAP in *G. obscuriglobus* cells was visualized by immunoelectron microscopy, probing with anti–RNAP-β primary antibody and a 10-nm gold-conjugated goat anti-mouse secondary antibody (Fig. 3*A*). RNAP-β was

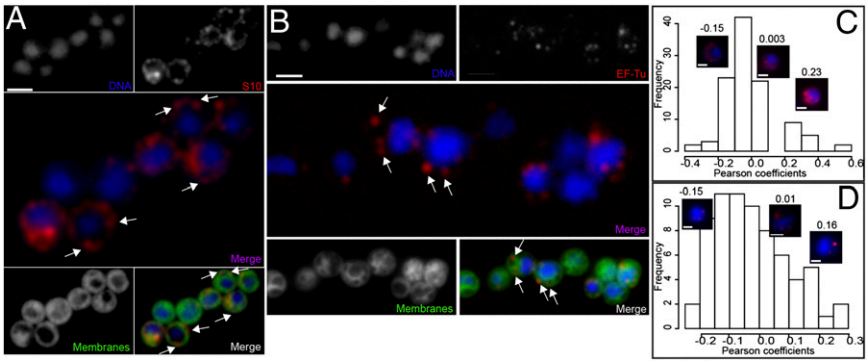

Fig. 2. Immunofluorescence microscopy detects translating ribosomes in both nucleoid-proximal and nucleoid-distal regions of the *G. obscuriglobus* cell. Quantitative colocalization analysis suggests enrichment of translating ribosomes in nucleoid-distal regions. (*A* and *B*) DNA is stained with DAPI; S10 (*A*) or EF-Tu (*B*) primary antibody is stained with Texas Red-conjugated secondary antibody; the merged image (purple) shows merged images of DAPI + S10 (*A*) or EF-Tu antibody (*B*). Membranes are stained with DiOC6. The merged image (white) shows DAPI + S10 (*A*) or EF-Tu antibody (*B*) + DiOC6. (*A*) S10 appears to be enriched in nucleoid-distal regions, with a punctate distribution. Arrows indicate ribosomes that are located distantly from the nucleoid and are localized to regions outlined by the DiOC6 membrane stain. (Scale bar: 2 μm.) (*B*) EF-Tu localization is similar to that of S10, being detected mostly in nucleoid-distal regions, with punctate distribution. Arrows indicate ribosomes that are distant from the nucleoid and are localized to regions outlined by the DiOC6 membrane stain. (Scale bar: 2 μm.) (*C* and *D*) For both anti-S10 and anti–EF-TU antibodies, the mean correlation coefficient falls around zero, and the majority of coefficients fall below the 0.5 threshold for positive colocalization of either S10 or EF-Tu with DAPI (0.01 ± 0.16 for S10 and −0.02 ± 0.12 for EF-Tu). Images were subjected to background subtraction across the entire image plane to eliminate false colocalization signals. (*C*) Colocalization analysis for S10 and DNA. Distribution of Pearson correlation coefficients for colocalization of signals from DAPI and anti-S10 antibody; $n = 126$ cells. Fluorescent images for three individual cells representative of the range of coefficients are provided. (Scale bars: 1 μm.) (*D*) Colocalization analysis for EF-Tu and DNA. Distribution of Pearson correlation coefficients for colocalization of signals from DAPI and anti–EF-Tu antibody; $n = 74$ cells. Fluorescent images for three individual cells representative of the range of coefficients are provided. (Scale bars: 1 μm.)

localized to the nucleoid(s) of *G. obscuriglobus*, with gold nanoparticles grouped in one to three clusters per nucleoid. RNAP was concentrated in the nucleoid central region, as also has been described in *B. subtilis* (4).

Use of Immunoelectron Microscopy and an Antibody-Independent Approach Support the Presence of Active Translation in Cellular Regions Distant from the Nucleoid(s). To permit higher-resolution localization, we performed immunoelectron microscopy using anti-S10 or anti–EF-Tu primary antibodies and a 15-nm gold-conjugated secondary antibody. We also used an antibody targeting dsDNA (and a corresponding secondary antibody conjugated to a smaller gold particle) in both single- and dual-labeling experiments. Use of the anti-dsDNA antibody alone (Fig. 3*B*) confirmed that it efficiently labeled the condensed nucleoid(s) typical of *G. obscuriglobus* (Fig. 1 refs. 10, 14, and 30). The scattered distribution of DNA signal outside the nucleoid(s) most likely is caused by nonspecific interactions of the antibody with proteins and RNA (Fig. S8).

We proceeded to use the anti-DNA antibody (rather than that targeting RNAP) as a proxy marker for transcription in dual-labeling experiments aiming to determine the spatial separation between transcription and translation, because the nucleoid labeled with the anti-DNA antibody occupies a greater cell area than the actively transcribing regions identified with the anti-RNAP antibody (Fig. 3 *A* and *B*). This approach thus could be expected to avoid overestimating the spatial segregation of transcription and translation. In dual-labeling experiments (Fig. 3 *C* and *D*), as in our fluorescence studies, we observed the larger gold nanoparticles indicating the location of S10 and EF-Tu throughout the cell. However, we did not detect significant enrichment of these proteins in particular regions of the cell (Table S1). Immunogold localization of translation markers in combination with electron tomography may be needed to obtain more definitive information about the relative amounts of translation occurring close to and distant from the nucleoid(s).

We also performed fluorescent labeling of ribosomes with gentamicin sulfate conjugated to the succinimidyl ester of Texas Red fluorescent dye (GTTR) (31), which is a previously unused application of this reagent. Because the aminoglycoside antibiotic gentamicin binds to the 16S ribosomal RNA on the 30S small ribosomal subunit A site of the assembled ribosome (32), it provides a convenient alternative marker of active translation. After exposure of *G. obscuriglobus* cells to GTTR, we observed Texas Red signal only in regions distant from the nucleoid(s) (Fig. 4*A*), as also seen in *Saccharomyces cerevisiae* (Fig. 4*B*). The relatively uniform distribution of GTTR signal provided a contrast to the punctate signal obtained with antibodies and suggests that gentamicin has an effect on ribosomal distribution. This notion is supported by our finding that the anti-S10 signal was distributed more uniformly in the presence of gentamicin (Fig. S9) than in its absence (Fig. 2*A*). The altered ribosomal distribution in the presence of gentamicin could be caused by cell-fixation artifacts (33), gentamicin-induced cellular stress (34, 35), a reduction in the ribosome recycling rate (36), or an increase in the ratio of monosomes to polysomes (37).

Discussion

Previous reports of highly unusual cellular ultrastructure in *G. obscuriglobus*, featuring a complex endomembrane system (10, 11, 13, 14) led us to test the hypothesis (12) that a substantial proportion of *G. obscuriglobus* translation may be spatially segregated from transcription. Before testing our hypothesis, we demonstrated that, in our hands, *G. obscuriglobus* cultures do indeed exhibit the previously reported cellular complexity.

The restricted distribution of RNAP-β as a transcription marker within nucleoid-proximal regions suggests that, as expected, these regions are the only sites of active transcription. The localization of RNAP-β in foci is consistent with the distribution reported for *B. subtilis* (4) but contrasts with its distribution in *E. coli* (6). The relationship between RNAP distribution, gene-expression level, and the spatial organization of transcription and translation in these organisms is not yet clear.

We showed that anti-S10 and anti–EF-Tu antibodies could be effective reagents for detecting translation. S10 can be found in both fully and partially assembled ribosomes (38), whereas EF-Tu can be bound only to an assembled ribosome (22) and thus is a better indicator of active protein synthesis. Further

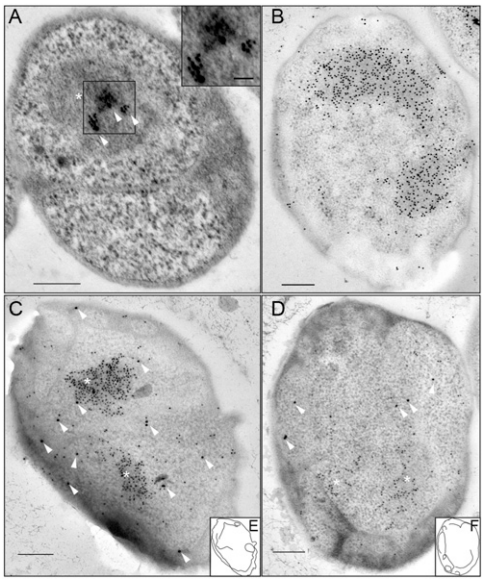

Fig. 3. Fibrillar bodies within cells of *G. obscuriglobus* were confirmed as nucleoids, and the site of transcription foci was determined by using antibodies targeting dsDNA and the RNAP-β subunit, respectively. Translating ribosomes were detected in both the nucleoid-proximal and nucleoid-distal regions through immunoelectron microscopy. Quantitative data are provided in Table S1. (Scale bars: 200 nm.) (*A*) Arrowheads indicate the location of gold-conjugated goat anti-mouse secondary antibodies binding to the anti-RNAP mouse monoclonal antibody. The *Inset* shows an enlarged view of gold nanoparticles. (*Inset*, scale bar: 50 nm.) A prominent internal membrane appears to be double-layered and to carry bound ribosomes, as previously reported (10). (*B*) The nucleoid is clearly labeled by a mouse primary anti-dsDNA antibody, followed by gold-conjugated goat anti-mouse secondary antibodies. (*C* and *D*) The nucleoid is labeled with anti-dsDNA antibody (small particles). Arrowheads indicate large particles corresponding to gold-conjugated goat anti-mouse secondary antibodies binding to the anti-S10 antibody (*C*) or anti–EF-Tu antibody (*D*). *E* and *F* show the outline of cellular membranes in *C* and *D*, respectively. Asterisks indicate the nucleoid(s) in *A*, *C*, and *D*.

evidence for the suitability of EF-Tu as a translation marker in exponential growth is that EF-Tu is colocalized with ribosomes during this growth phase in *B. subtilis* (39). We showed that both the anti-S10 and anti–EF-Tu antibodies could bind to ribosome-enriched cellular fractions. Although S10 was clearly enriched in the P2 fraction, EF-Tu was distributed more broadly. This broader distribution could be caused by the separation of EF-Tu from the ribosome during fractionation (40), the role of EF-Tu in cellular processes other than translation (41, 42), or cross-contamination of fractions revealed by this abundant protein (43). However, the binding of ribosome-enriched cellular fractions by anti-S10 and anti–EF-Tu antibodies allowed subsequent application of the antibodies to localize transcription and translation via immunomicroscopy (in which fraction cross-contamination is not a concern).

Both immunofluorescence and immunoelectron microscopy detected S10 and EF-Tu both proximal to and distant from the cell's nucleoid(s), with the fluorescence data showing a quantitatively greater proportion in distant regions. Although we recognize the resolution limitations of fluorescence microscopy for bacteria, we propose that this concern is somewhat mitigated when fluorescence and electron microscopy data are mutually supportive, as they are in this case. The observed distribution suggests similarities between the spatial organization of active translation in *G. obscuriglobus* and that seen in *E. coli* and *B. subtilis* (4, 6). Inhibition of translation by antibiotic treatment produced a change in EF-Tu distribution in *G. obscuriglobus* cells, confirming that EF-Tu participates in active translation. The punctate distribution of fluorescent signal for both S10 and EF-Tu may result from the majority of ribosomes occurring as polysomes (44–47). However, variations in cytoplasmic mRNA density cannot be excluded.

Use of an antibody-independent approach, i.e., GTTR, showed enrichment of translationally active ribosomes distant from the nucleoid(s), supporting conclusions drawn from immunofluorescence data. Depletion of polysomes in GTTR-treated cells may have shifted the apparent distribution of ribosomes from punctate to more uniform. Sequential treatment of *G. obscuriglobus* cells with gentamicin followed by anti-S10 antibody showed a more uniform, less punctate distribution of S10 than seen in cells without gentamicin, lending some support to polysome depletion as a cause of the discrepancy in signal distribution.

Our accumulated microscopy data suggest that *G. obscuriglobus* carries out both translation that is proximal to the nucleoid and thus is likely to be coupled with transcription (although we have no direct evidence of this coupling) and translation that is spatially segregated from transcription. However, both qualitative evaluation of the distribution of translation markers and quantitative analysis of colocalization suggest that translation is enriched in regions distant from the nucleoid(s). If this conclusion is supported by future work, several alternative mechanisms for provision of mRNAs to distal ribosomes could be proposed.

Elements of the nucleoid could "loop out" through cytoplasmic connections between cellular regions proximal to and distant from the nucleoid(s), such as those recently visualized by 3D electron tomography (17), permitting conventional coupled transcription and translation. More specifically, the proposed nucleoid organization of *G. obscuriglobus* (30) suggests that coiled DNA forms a hollow rod, a solenoidal structure, that can be bent and twisted to form a periodically ordered condensed nucleoid. Thus, the nucleoid may be able to penetrate the narrow interconnections between cellular compartments in *G. obscuriglobus.* This scenario is related to the proposed role of nucleoid expansion and the transertion mechanism in coupling transcription to translation (48).

G. obscuriglobus also could chaperone mRNAs to distal ribosomes in a manner similar to that proposed for *B. subtilis* (49). Alternatively, *G. obscuriglobus* may distribute mRNAs to distal translation sites by simple diffusion as in *E. coli* (8, 50). However, we anticipate that the *G. obscuriglobus* endomembrane network

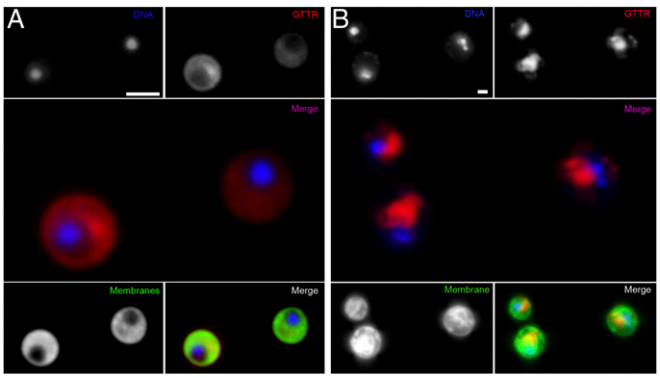

Fig. 4. The distribution of GTTR in cells of *G. obscuriglobus* is consistent with the spatial segregation of translation from the nucleoid. DNA is stained by DAPI. GTTR shows GTTR fluorescent labeling of actively translating ribosomes; the merged image (purple) shows a merged image of DAPI + GTTR. The membrane is stained with DiOC6. The merged image (white) shows a merged image of DAPI + GTTR + DiOC6. (Scale bar: 2 μm.) In *G. obscuriglobus*, the GTTR signal is observed in nucleoid-distal regions (*A*), as it is in the yeast *S. cerevisiae*, where the nuclear envelope serves to segregate translation spatially from the nucleoid (*B*).

would create obstacles to mRNA diffusion or would increase the diffusion distances to an extent that impedes protein synthesis. We do not currently have experimental evidence supporting this speculation.

Last, it is conceivable that *G. obscuriglobus* possesses specialized mRNA trafficking mechanisms, perhaps connected to the endomembrane system. An intriguing aspect of this last proposal is the reported presence in *G. obscuriglobus* and its relatives of proteins that structurally resemble membrane coat proteins (51), such as clathrins and nucleoporins. One representative of these proteins has been localized to *G. obscuriglobus* endomembranes (16, 51).

We have presented evidence that in the endomembrane-containing planctomycete species *G. obscuriglobus*, a substantial proportion of active translation likely occurs in regions distant from the nucleoid(s). Our findings have emerged at an interesting time for our understanding of informational macromolecular processing in bacterial cells. Although dogma maintains that most bacterial transcription and translation are directly coupled, recent studies in *E. coli* and *B. subtilis* provide evidence for considerable spatial segregation. However, the *G. obscuriglobus* cell presents an additional layer of organizational complexity relative to these organisms, namely an endomembrane system. We thus report the first evidence, to our knowledge, for spatially segregated transcription and translation in a bacterial cell in which the cytoplasmic volume is convoluted by the presence of membranes that impose considerable distance between the nucleoid(s) and peripheral ribosomes. Our study broadens the understanding of the diversity in spatial organization of bacterial gene expression, which currently is based entirely on a handful of model species. Our results also suggest (but do not directly demonstrate) that endomembranes may provide an obstacle to colocated transcription and translation, a role for endomembranes that has not been reported previously for a prokaryotic organism. This work provides a useful background for consideration of the evolutionary development of eukaryotic cellular complexity and how it led to decoupled processes of gene expression in eukaryotes.

Materials and Methods

Microbial Strains and Growth. *Gemmata obscuriglobus* DSM5831^T was obtained from the Deutsche Sammlung von Mikroorganismen und Zellkulturen (Braunschweig, Germany) and grown in standard planctomycete medium (52, 53). *Escherichia coli* UCLA #1246 was received from Erin Sanders (University of California, Los Angeles), and *Saccharomyces cerevisiae* wild-type strain PTY44 was provided by Peter Thorsness (University of Wyoming, Laramie, WY). Specific conditions for culture growth and treatment with gentamicin, GTTR, and chloramphenicol are described in *SI Materials and Methods*.

Antibodies and Custom Antibody Design. The RNAP-β antibody (ab81865; Abcam) was a Protein G-purified mouse monoclonal (8RB13) raised vs. the full-length *E. coli* RNAP-β subunit. The anti-dsDNA antibody (ab27156; Abcam) was a Protein A-purified mouse monoclonal (HYB331-01) raised against dsDNA. Secondary antibody conjugates included goat anti-rabbit IgG-HRP antibody (A0545; Sigma), goat anti-mouse IgG/IgM-HRP antibody (AR103P; Chemicon), goat anti-rabbit IgG (H + L)-Texas Red antibody (T6391; Molecular Probes, Life Technologies), goat anti-mouse IgG polyclonal-10 nm gold antibody and goat anti-rabbit IgG polyclonal-15 nm gold antibody [EMS25129 and EMS25113; Electron Microscopy Sciences (EMS)].

Synthetic peptides and custom anti-peptide polyclonal antibodies were produced for the *G. obscuriglobus* proteins S10 (ZP_02734663; full-length protein, 110 aa), EF-Tu (ZP_02733080; full-length protein, 434 aa), and NusG (ZP_02733082; full-length protein, 223 aa) by Pierce Biotechnology, Inc./Thermo Fisher Scientific. Antibody production and Western blot analysis are described in *SI Materials and Methods*.

Ribosome Isolation and Analysis. The ribosomal isolation procedure was adapted from that of Ban et al. (54) and Moore et al. (55). Fraction preparation, nucleic acid and protein content analyses, and Western blot analysis are described in *SI Materials and Methods*.

Immunofluorescence. *G. obscuriglobus* was grown on M1 agar to exponential phase, and harvested cells were washed two times in PBS. Cells were fixed in 0.5 mL 40 mg/ml paraformaldehyde (Sigma) in PBS for 10 min, followed by three PBS washes. Cells then were permeabilized with cold acetone (−20 °C) for 10 min and washed three times with PBS. Samples were blocked in blocking buffer [10 mg/ml milk/PBS/0.05%Tween-20 (10 mg/ml milk/TPBS)] for 1 h at room temperature and were probed with the appropriate primary antibody (1:10 dilution) in blocking buffer for 1 h at room temperature. Specimens were washed three times for 15 min with TPBS and then were probed with goat anti-rabbit Texas Red secondary antibody (T6391, 1:500 dilution in 10 mg/ml milk/TPBS) for 1 h at room temperature. Two further 15-min washes with TPBS and one final 15-min wash with PBS were performed. During the last wash, 1 μg each of DAPI (Invitrogen) and DiOC6 (Molecular Probes) was added per milliliter of sample. Cells were washed three times for 5 min with PBS to remove excess fluorescent dyes. Cells then were mounted on clean glass slides 1:1 with 20 mg/ml low melting agarose (Bio-Rad) solution in PBS.

High-Pressure Freezing and Cryosubstitution. Cryofixation and freeze substitution (FS) for both ultrastructure and immunoelectron microscopy were performed at the Molecular, Cellular, and Developmental Biology Electron Microscopy Facility, University of Colorado-Boulder, using a previously described method (56). Exponentially growing *G. obscuriglobus* cultures (OD_{600} 0.4–0.6; grown for 5 d in Deutsche Sammlung von Mikroorganismen und Zellkulturen 629 liquid medium) were used for FS and further immunogold labeling. Experimental details for FS are described in *SI Materials and Methods*.

Immunogold Labeling. When necessary, enzymatic digestion was performed on thin sections using a procedure modified from that of Bohrmann and Kellenberger (57); experimental details are described in *SI Materials and Methods*. Thin sections were blocked in 50 mg/ml normal boiled donkey serum solution diluted in PHEM buffer [60 mM piperazine-*N*,*N*′-bis(2-ethanesulfonic acid), 25 mM 4-(2-hydroxyethyl)-1-piperazineethanesulfonic acid, 10 mM ethylene glycol tetraacetic acid, 2 mM MgCl2, pH 6.5] (Jackson ImmunoResearch Laboratories) in PBS for 1 h at room temperature, incubated for 1.5 h in primary antibody solution (1:10 in blocking buffer), and rinsed three times for 15 min with TPBS. Sections then were incubated in the appropriate gold-conjugated secondary antibody(s) solution (1:10 or 1:2.5 in blocking buffer) followed by two TPBS rinses for 15 min and one PBS rinse for 10 min. For double-antibody labeling, both primary and both secondary antibodies were added to the incubation solution simultaneously. Sections were incubated for 1 h in double-antibody solutions and rinsed as described above. Staining, drying, and storage were performed as described for ultrastructure studies in *SI Materials and Methods*.

Cell Imaging. Fluorescent microscopy was carried out using an Olympus IX71 inverted microscope equipped with Ludl excitation and emission filter wheels and shutters. Images were acquired at room temperature using a 100× 1.4 NA objective (with 1.6× optivar) and an Orca Flash 2.8 scientific cMOS camera (Hamamatsu). Microscope components and automation were controlled using Metamorph software (Molecular Devices). Ultrastructure and immunogold-labeled images were acquired using a transmission electron microscope (Hitachi H-7000) at 75 kV, a Gatan digital camera, and Gatan software. Fluorescent and electron microscopy images were processed (when specified) and analyzed with ImageJ (National Institutes of Health) and Adobe Illustrator CS6. At least 20 cells were analyzed for each fluorescent, immunofluorescent, and immunoelectron microscopy experiment, and representative images were chosen that depict the most common cellular features. Each fluorescent-channel micrograph was taken with the same exposure time. Level and brightness adjustments were applied across the entire images in blue, green, and red channels to clarify important features.

Colocalization and Statistical Analysis. Colocalization analysis for fluorescence microscopy was performed with ImageJ software using the "Intensity colocalization analysis" plug-in with default parameters (58). This method of colocalization analysis is used frequently in cell biology (59, 60). Image processing and statistical analysis for both fluorescent and electron microscopy are described further in *SI Materials and Methods*.

ACKNOWLEDGMENTS. We thank Zhaojei Zhang (University of Wyoming) and Thomas Giddings (University of Colorado Molecular, Cellular, and Developmental Biology EM Service) and his research group for assistance with TEM studies and Grant Bowman, Heather Rothfuss, David Liberles (all University of Wyoming), Olga Kamneva (University of California, Berkeley), and Patrick LaBreck (Uniformed Services University) for helpful discussions. This

work was supported by US National Science Foundation Award MCB-0920667 (to N.L.W.), National Center for Research Resources Grant 5P20RR016474-12, and National Institute of General Medical Sciences, National Institutes of Health Grant 8 P20 GM103432-12.

1. Gowrishankar J, Harinarayanan R (2004) Why is transcription coupled to translation in bacteria? *Mol Microbiol* 54(3):598–603.
2. Miller OL, Hamkalo BA, Thomas CA (1970) Visualization of Bacterial Genes in Action. *Science* 169(3943):392–395.
3. Montero Llopis P, et al. (2010) Spatial organization of the flow of genetic information in bacteria. *Nature* 466(7302):77–81.
4. Lewis PJ, Thaker SD, Errington J (2000) Compartmentalization of transcription and translation in Bacillus subtilis. *EMBO J* 19(4):710–718.
5. Mascarenhas J, Weber MH, Graumann PL (2001) Specific polar localization of ribosomes in Bacillus subtilis depends on active transcription. *EMBO Rep* 2(8):685–689.
6. Azam TA, Hiraga S, Ishihama A (2000) Two types of localization of the DNA-binding proteins within the Escherichia coli nucleoid. *Genes Cells* 5(8):613–626.
7. Mondal J, Bratton BP, Li Y, Yethiraj A, Weisshaar JC (2011) Entropy-based mechanism of ribosome-nucleoid segregation in E. coli cells. *Biophys J* 100(11):2605–2613.
8. Nevo-Dinur K, Nussbaum-Shochat A, Ben-Yehuda S, Amster-Choder O (2011) Translation-independent localization of mRNA in E. coli. *Science* 331(6020):1081–1084.
9. Franzmann PD, Skerman VBD (1984) Gemmata obscuriglobus, a new genus and species of the budding bacteria. *Antonie van Leeuwenhoek* 50(3):261–268.
10. Fuerst JA, Webb RI (1991) Membrane-bounded nucleoid in the eubacterium Gemmata obscuriglobus. *Proc Natl Acad Sci USA* 88(18):8184–8188.
11. Fuerst JA (1995) The planctomycetes: Emerging models for microbial ecology, evolution and cell biology. *Microbiology* 141(Pt 7):1493–1506.
12. Fuerst JA (2005) Intracellular compartmentation in planctomycetes. *Annu Rev Microbiol* 59:299–328.
13. Lindsay MR, et al. (2001) Cell compartmentalisation in planctomycetes: Novel types of structural organisation for the bacterial cell. *Arch Microbiol* 175(6):413–429.
14. Lieber A, Leis A, Kushmaro A, Minsky A, Medalia O (2009) Chromatin organization and radio resistance in the bacterium Gemmata obscuriglobus. *J Bacteriol* 191(5): 1439–1445.
15. Fuerst JA, Sagulenko E (2010) Protein uptake by bacteria: An endocytosis-like process in the planctomycete Gemmata obscuriglobus. *Commun Integr Biol* 3(6):572–575.
16. Acehan D, Santarella-Mellwig R, Devos DP (2013) A bacterial tubulovesicular network. *J Cell Sci*.
17. Santarella-Mellwig R, Pruggnaller S, Roos N, Mattaj IW, Devos DP (2013) Three-dimensional reconstruction of bacteria with a complex endomembrane system. *PLoS Biol* 11(5):e1001565.
18. Sagulenko E, et al. (2014) Structural studies of planctomycete Gemmata obscuriglobus support cell compartmentalisation in a bacterium. *PLoS ONE* 9(3):e91344.
19. Lonhienne TGA, et al. (2010) Endocytosis-like protein uptake in the bacterium Gemmata obscuriglobus. *Proc Natl Acad Sci USA* 107(29):12883–12888.
20. Fuerst JA, Sagulenko E (2012) Keys to eukaryality: Planctomycetes and ancestral evolution of cellular complexity. *Front Microbiol* 3. Available at: www.ncbi.nlm.nih.gov/pmc/articles/PMC3343278/. accessed December 3, 2012.
21. McInerney JO, et al. (2011) Planctomycetes and eukaryotes: A case of analogy not homology. *BioEssays* 33(11):810–817.
22. Devos DP (2012) Regarding the presence of membrane coat proteins in bacteria: Confusion? What confusion? *BioEssays* 34(1):38–39.
23. Kaziro Y (1978) The role of guanosine 5′-triphosphate in polypeptide chain elongation. *Biochim Biophys Acta* 505(1):95–127.
24. Lucas-Lenard J, Lipmann F (1971) Protein biosynthesis. *Annu Rev Biochem* 40:409–448.
25. Pape T, Wintermeyer W, Rodnina MV (1998) Complete kinetic mechanism of elongation factor Tu-dependent binding of aminoacyl-tRNA to the A site of the E. coli ribosome. *EMBO J* 17(24):7490–7497.
26. Schmidt RJ, Myers AM, Gillham NW, Boynton JE (1984) Chloroplast ribosomal proteins of Chlamydomonas synthesized in the cytoplasm are made as precursors. *J Cell Biol* 98(6):2011–2018.
27. Burmann BM, Rösch P (2011) The role of E. coli Nus-factors in transcription regulation and transcription:translation coupling: From structure to mechanism. *Transcription* 2(3):130–134.
28. Zinchuk V, Zinchuk O, Okada T (2007) Quantitative colocalization analysis of multicolor confocal immunofluorescence microscopy images: Pushing pixels to explore biological phenomena. *Acta Histochem Cytochem* 40(4):101–111.
29. Manders EM, Stap J, Brakenhoff GJ, van Driel R, Aten JA (1992) Dynamics of three-dimensional replication patterns during the S-phase, analysed by double labelling of DNA and confocal microscopy. *J Cell Sci* 103(Pt 3):857–862.
30. Yee B, Sagulenko E, Morgan GP, Webb RI, Fuerst JA (2012) Electron tomography of the nucleoid of Gemmata obscuriglobus reveals complex liquid crystalline cholesteric structure. *Front Microbiol* 3. Available at: www.ncbi.nlm.nih.gov/pmc/articles/PMC3440768/. accessed December 3, 2012.
31. Wang Q, Steyger PS (2009) Trafficking of systemic fluorescent gentamicin into the cochlea and hair cells. *J Assoc Res Otolaryngol* 10(2):205–219.
32. Yoshizawa S, Fourmy D, Puglisi JD (1998) Structural origins of gentamicin antibiotic action. *EMBO J* 17(22):6437–6448.
33. Escobedo JO, Chu Y-H, Wang Q, Steyger PS, Strongin RM (2012) Live cell imaging of a fluorescent gentamicin conjugate. *Nat Prod Commun* 7(3):317–320.
34. Tenson T, Mankin A (2006) Antibiotics and the ribosome. *Mol Microbiol* 59(6): 1664–1677.
35. Mehta R, Champney WS (2003) Neomycin and paromomycin inhibit 30S ribosomal subunit assembly in Staphylococcus aureus. *Curr Microbiol* 47(3):237–243.
36. Borovinskaya MA, et al. (2007) Structural basis for aminoglycoside inhibition of bacterial ribosome recycling. *Nat Struct Mol Biol* 14(8):727–732.
37. Eustice DC, Wilhelm JM (1984) Fidelity of the eukaryotic codon-anticodon interaction: Interference by aminoglycoside antibiotics. *Biochemistry* 23(7):1462–1467.
38. Wimberly BT, et al. (2000) Structure of the 30S ribosomal subunit. *Nature* 407(6802): 327–339.
39. Defeu Soufo HJ, et al. (2010) Bacterial translation elongation factor EF-Tu interacts and colocalizes with actin-like MreB protein. *Proc Natl Acad Sci USA* 107(7): 3163–3168.
40. Trauner A, Bennett MH, Williams HD (2011) Isolation of bacterial ribosomes with monolith chromatography. *PLoS ONE* 6(2):e16273.
41. Granato D, et al. (2004) Cell surface-associated elongation factor Tu mediates the attachment of Lactobacillus johnsonii NCC533 (La1) to human intestinal cells and mucins. *Infect Immun* 72(4):2160–2169.
42. Kolberg J, et al. (2008) The surface-associated elongation factor Tu is concealed for antibody binding on viable pneumococci and meningococci. *FEMS Immunol Med Microbiol* 53(2):222–230.
43. Kunze G, et al. (2004) The N terminus of bacterial elongation factor Tu elicits innate immunity in Arabidopsis plants. *Plant Cell* 16(12):3496–3507.
44. Slayter H, Kiho Y, Hall C, Rich A (1968) An electron microscopic study of large bacterial polyribosomes. *J Cell Biol* 37(2):583–590.
45. Kennell D, Riezman H (1977) Transcription and translation initiation frequencies of the Escherichia coli lac operon. *J Mol Biol* 114(1):1–21.
46. Bliska JB, Cozzarelli NR (1987) Use of site-specific recombination as a probe of DNA structure and metabolism in vivo. *J Mol Biol* 194(2):205–218.
47. Brandt F, et al. (2009) The native 3D organization of bacterial polysomes. *Cell* 136(2): 261–271.
48. Woldringh CL (2002) The role of co-transcriptional translation and protein translocation (transertion) in bacterial chromosome segregation. *Mol Microbiol* 45(1): 17–29.
49. El-Sharoud WM, Graumann PL (2007) Cold shock proteins aid coupling of transcription and translation in bacteria. *Sci Prog* 90(Pt 1):15–27.
50. Bakshi S, Siryaporn A, Goulian M, Weisshaar JC (2012) Superresolution imaging of ribosomes and RNA polymerase in live Escherichia coli cells. *Mol Microbiol* 85(1): 21–38.
51. Santarella-Mellwig R, et al. (2010) The compartmentalized bacteria of the planctomycetes-verrucomicrobia-chlamydiae superphylum have membrane coat-like proteins. *PLoS Biol* 8(1):e1000281, Available at: www.ncbi.nlm.nih.gov/pmc/articles/PMC2799638/. Accessed March 1, 2013.
52. Staley JT (1973) Budding bacteria of the Pasteuria-Blastobacter group. *Can J Microbiol* 19(5):609–614.
53. Falkow S, Rosenberg E, Schleifer K-H, Stackebrandt E (2006) *The Prokaryotes-Proteobacteria: Delta and Epsilon Subclasses. Deeply Rooting Bacteria* (Springer, Singapore) Vol. 7.
54. Ban N, Nissen P, Hansen J, Moore PB, Steitz TA (2000) The complete atomic structure of the large ribosomal subunit at 2.4 A resolution. *Science* 289(5481):905–920.
55. Moore SD, Baker TA, Sauer RT (2008) Forced extraction of targeted components from complex macromolecular assemblies. *Proc Natl Acad Sci USA* 105(33):11685–11690.
56. Giddings TH (2003) Freeze-substitution protocols for improved visualization of membranes in high-pressure frozen samples. *J Microsc* 212(Pt 1):53–61.
57. Bohrmann B, Kellenberger E (1994) Immunostaining of DNA in electron microscopy: An amplification and staining procedure for thin sections as alternative to gold labeling. *J Histochem Cytochem* 42(5):635–643.
58. Li Q, et al. (2004) A syntaxin 1, Galpha(o), and N-type calcium channel complex at a presynaptic nerve terminal: Analysis by quantitative immunocolocalization. *J Neurosci* 24(16):4070–4081.
59. French AP, Mills S, Swarup R, Bennett MJ, Pridmore TP (2008) Colocalization of fluorescent markers in confocal microscope images of plant cells. *Nat Protoc* 3(4): 619–628.
60. Panyasrivanit M, Khakpoor A, Wikan N, Smith DR (2009) Co-localization of constituents of the dengue virus translation and replication machinery with amphisomes. *J Gen Virol* 90(Pt 2):448–456.